plants

MDPI

Article

4-Hydroxybenzoic Acid as an Antiviral Product from Alkaline Autoxidation of Catechinic Acid: A Fact to Be Reviewed

Silvana Alfei [1,*], Debora Caviglia [2,*], Susanna Penco [3], Guendalina Zuccari [1] and Fabio Gosetti [4]

[1] Department of Pharmacy (DIFAR), University of Genoa, Viale Cembrano, 4-16148 Genoa, Italy; zuccari@difar.unige.it
[2] Department of Surgical Sciences and Integrated Diagnostics (DISC), University of Genoa, Viale Benedetto XV, 6-16132 Genoa, Italy
[3] Department of Experimental Medicine, University of Genoa, Via Leon Battista Alberti, 2-16132 Genoa, Italy; susanna.penco@unige.it
[4] Department of Earth and Environmental Sciences (DISAT), University of Milano-Bicocca, Piazza della Scienza, 1-20126 Milano, Italy; fabio.gosetti@unimib.it
* Correspondence: alfei@difar.unige.it (S.A.); debora.caviglia@edu.unige.it (D.C.); Tel.: +39-010-355-2296 (S.A.)

Abstract: The dark brown mixture resulting from the autooxidation of catechinic acid (CA) (AOCA) has been reported to possess antiviral activity against Herpes Simplex Virus 1 and 2 (HSV-1 and HSV-2). Unfortunately, the constituents of AOCA were not separated or identified and the compound(s) responsible for AOCA's antiviral activity remained unknown until recently. Colorless 4-hydroxy benzoic acid (4-HBA) has been reported as the main constituent (75%) of AOCA, and as being responsible for its antiviral activity. The findings seem not to be reliable because of the existence in the literature of very different findings, the high concentration that was attributed to the supposed 4-HBA in the dark mixture, and the insufficient or inaccurately interpreted analytical experiments reported in the study identifying 4-HBA in AOCA. Of particular concern is the lack of AOCA chromatograms highlighting a peak attributable to 4-HBA, using commercial 4-HBA as a standard, and investigations concerning the antiviral activity of marketed 4-HBA. Therefore, in this study, to verify the exactness of the recent reports, we prepared CA from catechin and AOCA from CA, and the absence of 4-HBA in the mixture was first established by thin-layer chromatography (TLC), and then was confirmed by UHPLC–MS/MS, UV–Vis, and ATR–FTIR analyses. For further confirmation, the ATR–FTIR spectral data were processed by principal components analysis (PCA), which unequivocally established strong structural differences between 4-HBA and AOCA. Finally, while the antiviral effects of AOCA against HSV-2 were confirmed, a commercial sample of 4-HBA was completely inactive.

Keywords: (+)-catechin; catechinic acid (CA); alkaline autooxidation of CA (AOCA); 4-hydroxybenzoic acid (4-HBA); antiviral activity; ultra-high-performance liquid chromatography (UHPLC); thin-layer chromatography (TLC); ultraviolet–visible spectroscopy (UV–Vis); attenuated total reflection Fourier transform infrared (ATR–FTIR); principal components analyses (PCA)

Citation: Alfei, S.; Caviglia, D.; Penco, S.; Zuccari, G.; Gosetti, F. 4-Hydroxybenzoic Acid as an Antiviral Product from Alkaline Autoxidation of Catechinic Acid: A Fact to Be Reviewed. *Plants* **2022**, *11*, 1822. https://doi.org/10.3390/plants11141822

Academic Editors: Ioan Grozescu and Maria Iorizzi

Received: 28 June 2022
Accepted: 8 July 2022
Published: 11 July 2022

1. Introduction

Infusions obtained with the leaves of *Combretum micranthum* G. Don (Combretaceae) are commonly used in the folk medicine of West Africa, for the treatment of various diseases [1,2]. As reported, the main constituents in this species are polyphenolic compounds, including *O*-glycosylflavones, *C*-glycosylflavones, flavans [1,3,4], and flavan-piperidine alkaloids (kinkéloids) [2].

In 1993, and later in 2000, it was reported that while a freshly prepared solution of the methanolic extract of *C. micranthum* leaves was inactive against the HSV-1 and HSV-2 viruses, the one-week-aged extract or the extract subjected to alkaline autoxidation was, instead, particularly active against the same viruses [5,6]. In this regard, it has been hypothesized that aging, catalyzed in an alkaline environment, combined with heating

at temperatures above 90 °C, would have been responsible for the formation of active compounds from the inactive precursors present in the extract [5]. Considering that catechins are the main constituents of the methanolic extract and that, in a hot alkaline solution, (+)-catechin undergoes rearrangement to catechinic acid (CA) (Figure 1) [7], Ferrea and coworkers prepared CA from pure (+)-catechin [5].

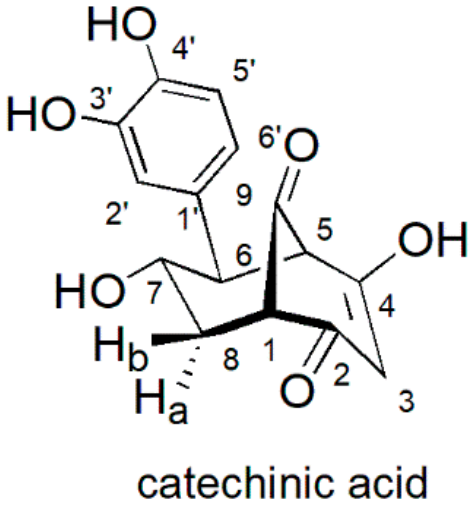

Figure 1. Structure and atom numbering of CA.

Subsequently, by the same group, the synthetized CA was oxidized in an alkaline oxygen-saturated solution at 100 °C, and the dark brown complex reaction mixture (AOCA) was chemically and biologically investigated [5]. Almost comparable antiherpetic activity and very similar IR and UV–Vis spectra of the alkaline oxidized methanolic extract and AOCA were observed, thus establishing that the oxidation products of CA were the main ones responsible for the antiviral activity in the oxidized extract [5]. Wishing to develop from AOCA a new antiviral agent, active against the viruses of the Herpes family, Ferrea and colleagues subsequently tried to isolate and identify the main component of AOCA, but unfortunately, they only succeeded in dividing AOCA into several fractions, all endowed with similar antiherpetic activity.

In a recent study [8], the main constituent (75%) of AOCA was isolated by Iobbi et al. (i.e., compound **2** in their work). It was identified as the colorless and well-known 4-hydroxy benzoic acid (4-HBA), and it was reported to be responsible for the antiviral activity of AOCA, as **2** had been found to be active on tomato brown rugose fruit virus (ToBRFV). Curiously, this finding turned out to be very different from what was already widely reported in several specific articles, some of which were cited by the authors of this study themselves, in a counterproductive way [9–13]. In this regard, the structural identity recently attributed to **2** was validated by Iobbi et al., since 4-HBA is commonly produced by the thermolytic degradation of some flavonoids [14,15]. However, it is possible to argue that the thermolytic conditions under which this occurs are considerably more drastic than those used by Iobbi and coworkers to produce AOCA. Moreover, it is known in the literature that 4-HBA derives only from flavonoids structurally different from catechin [14,15]. In particular, catechin, encompassing two catechol phenyl rings both having two hydroxyl groups, is very unlikely to thermolytically provide 4-HBA, which possesses only one hydroxyl group. In fact, the works cited by the authors to justify the presence of 4-HBA in AOCA report that 4-HBA derives from flavonoids with at least one phenyl ring having only one hydroxyl function, and whose structure can precisely degrade to 4-HBA [14,15]. In addition, while many flavonoids are known to degrade into simpler phenolic molecules, such as protocatechuic acid, phloroglucinol, 4-HBA, and caffeic acid, none of these compounds have been observed in the alkaline degradation of flavonoids that initially provide CA, such as catechin [16]. In practice, the CA resulting from the alkaline treatment of (+)-catechin has been shown to be sufficiently stable against further alkaline

transformation, to allow only the combination of two or more CA molecules and, therefore, permitting mainly the formation of dimers, in which the nucleus of CA is maintained [9,16]. In fact, while, through the initial formation of a quinone derivative, hydroxycatechinic and dehydrocatechinic acids and their dimers have been described as the main constituents of the product of the alkaline oxidation of CA obtainable under conditions such as those used to obtain AOCA, 4-HBA has not been isolated so far [9]. Additionally, the other compounds described by Laks et al. [10], Ohara et al. [11], and Hashida et al. [12,13], as originating from the alkaline degradation of CA, were not detected by Iobbi and coauthors [8]. Among other pivotal analyses missing in the article by Iobbi et al., a simple experiment to confirm the structural identity (4-HBA) attributed to **2** should have been performed, in the form of testing a commercial sample of 4-HBA on ToBRFV, confirming or refuting its identical antiviral activity, but such a test was not performed. Precisely for this purpose, we tested, as reported by Ferrea et al. in 1993, a commercial sample of 4-HBA on VERO cells infected with HSV-2 viruses, and discovered, unfortunately, that 4HBA was completely inactive. Therefore, also for this reason, the identity attributed to compound **2**, found active against ToBRFV, was unlikely, especially at the high concentration reported (75%). In addition, no chromatogram of AOCA that highlighted the presence of a peak attributable to 4-HBA, using a commercial sample of 4-HBA as a reference compound, has been provided by Iobbi et al. [8]. Therefore, without investigating the authors' ability to perform separation and isolation procedures—which is not within our competence—and without aiming at identifying the constituents of AOCA as well as its main component (if a main component in fact exists), responsible for its antiviral activity, we undertook this study to verify the accuracy of the identity attributed to the molecule (**2**) that the authors were able to separate. To this end, from (+)-catechin, CA was prepared, completely characterized, and oxidized to AOCA, according to procedures reported years ago [5,7] and re-performed in this recent study [8], and the possible presence of 4-HBA in the mixture was investigated by different analytical techniques. In particular, the absence of 4-HBA in the mixture was first established by thin-layer chromatography (TLC), and then was confirmed by UHPLC–MS/MS, UV–Vis, and ATR–FTIR analyses. Additionally, the ATR–FTIR spectral data were processed by principal components analysis (PCA), which unequivocally established strong structural differences between 4-HBA and AOCA, thus further confirming that AOCA does not contain 4-HBA. Finally, the antiviral effects of AOCA against HSV-2 were investigated and confirmed, thus establishing that the AOCA prepared by us, and not containing 4-HBA, is identical to the one recently reported by Iobbi et al and testified to contain 4-HBA, but whose activity against HSV-2 had not been verified.

2. Results and Discussion

2.1. Preparation of Catechinic Acid (CA)

CA was prepared as previously described [5,7,8,13], starting from commercial (+)-catechin according to Scheme 1, in which the numbering of atoms of catechin and CA has been reported, to facilitate an understanding of the mechanism of the reaction and to clarify the assignments reported in the peak lists of NMR analyses (Materials and Methods section). In this regard, we note that in the Supplementary Materials of the work by Iobbi et al., in which **2** was isolated, the structure of CA reported in Figure S1 is incorrect [8]. In fact, the catechol ring should be linked to C-6 and not to C-8, which should have two diastereotopic proton atoms, i.e., Ha and Hb (as reported in the ^{1}H-NMR peak list of both the present work and that of Iobbi et al.) and not one, as herein observable in Figure 1 and Scheme 1.

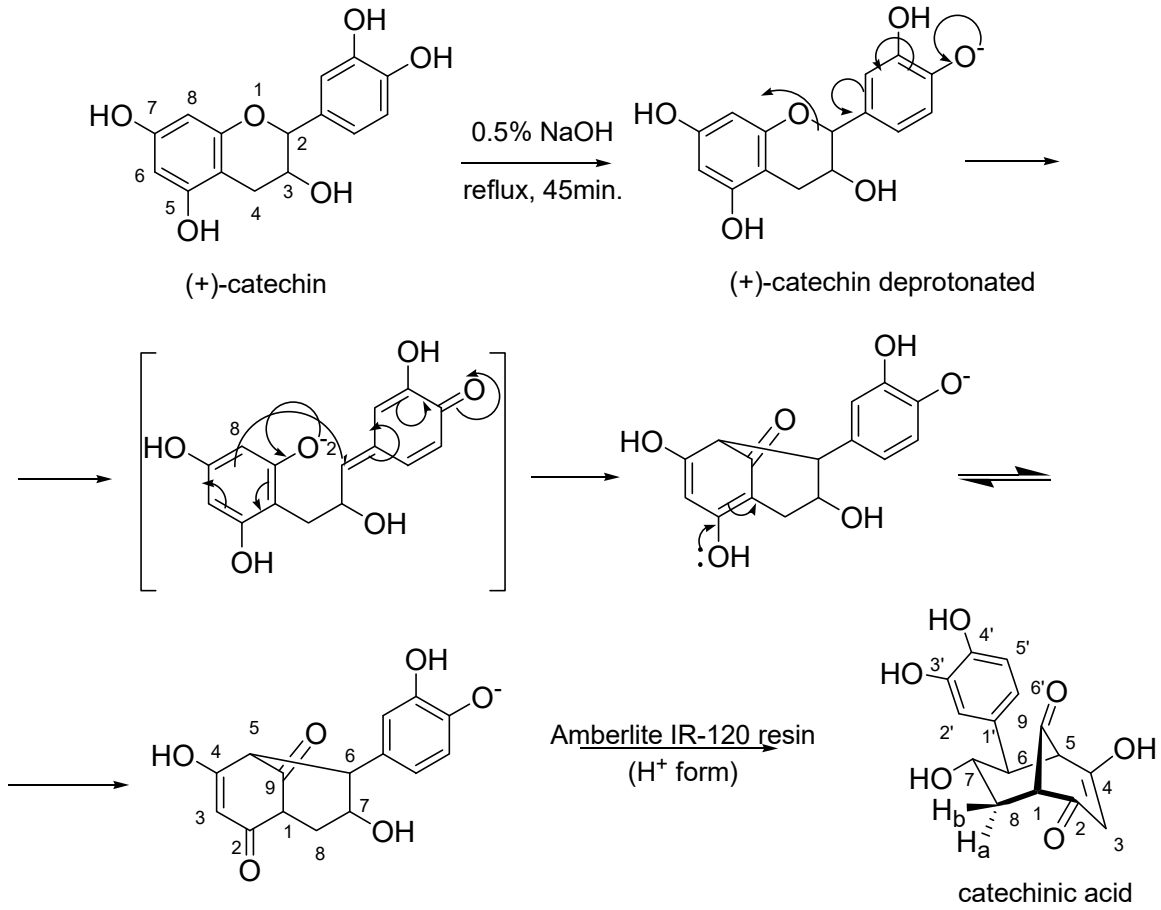

Scheme 1. Synthetic procedure and mechanism that lead to the obtainment of CA.

The reaction was followed by TLC, which allowed us to highlight the disappearance of the spot of (+)-catechin at Rf. 0.82 and the appearance of that of CA at Rf. 0.26. An image reporting the TLC of (+)-catechin and of the crude CA, of the isolated CA, and of three samples of CA recrystallized by acetone/Et_2O is available in Section S1 (SM), as Figure S1. Specifically, it has been reported [7,13] that the basic treatment of (+)-catechin at 25 °C provides enantiomeric epicatechin by epimerization at the C-2 position of the pyran ring, whereas CA is obtained when the same treatment is conducted at 100 °C [7,13,17]. These reactions are supposed to proceed both through the basic catalyzed cleavage of the pyran ring to give the quinone-methide intermediate, followed by the reclosure of the pyran ring affording epicatechin, or by the nucleophilic attack of the π doublet between C-7 and C-8 of the phenyl ring at the C-2 position of the quinone-methide intermediate to afford CA (Scheme 1). A radical reaction mechanism was proposed because these reactions are inhibited by the exclusion of oxygen [13,18]. Differently, Ohara and Hemingway showed that at an intermediate temperature (40 °C), the diarylpropanol-catechin acid dimer is produced together with catechin acid [11], and other unidentified compounds are produced in low yields [13]. Chemically, CA is an enolic form of 6-(3,4-dihydroxyphenyl)-7-hydroxybicyclo [3.3.1]-nonane-2,4,9-trione [13]. We obtained crude CA as a dark brown oil, and upon purification by fast filtration on a silica gel plug, followed by crystallization, we achieved highly pure CA as pale orange crystals (70% isolated yield) (Figure S2 in Section S1 of SM). Notably, extremely neat CA was achieved, without recovery via high-cost and long-term semi-preparative HPLC, which uses large amounts of solvents and requires expert workers and costly apparatus, as recently reported [8]. In our opinion, the use of special purification techniques when it is not strictly necessary is not a good practice in an academic laboratory, both in terms of costs and with respect to the environment. The structure of the obtained CA, which we isolated in a much simpler, cheaper, and faster manner, was

confirmed by ATR–FTIR (Figure 2) and ^{1}H and ^{13}C NMR spectroscopy (Figures S3 and S4 in Section S1 of SM), while its purity was assessed first by TLC (Figure S1, Section S1, SM), and then by UV–Vis and UHPLC–MS/MS analyses (Figures 3 and 4), and finally further confirmed by elemental analyses.

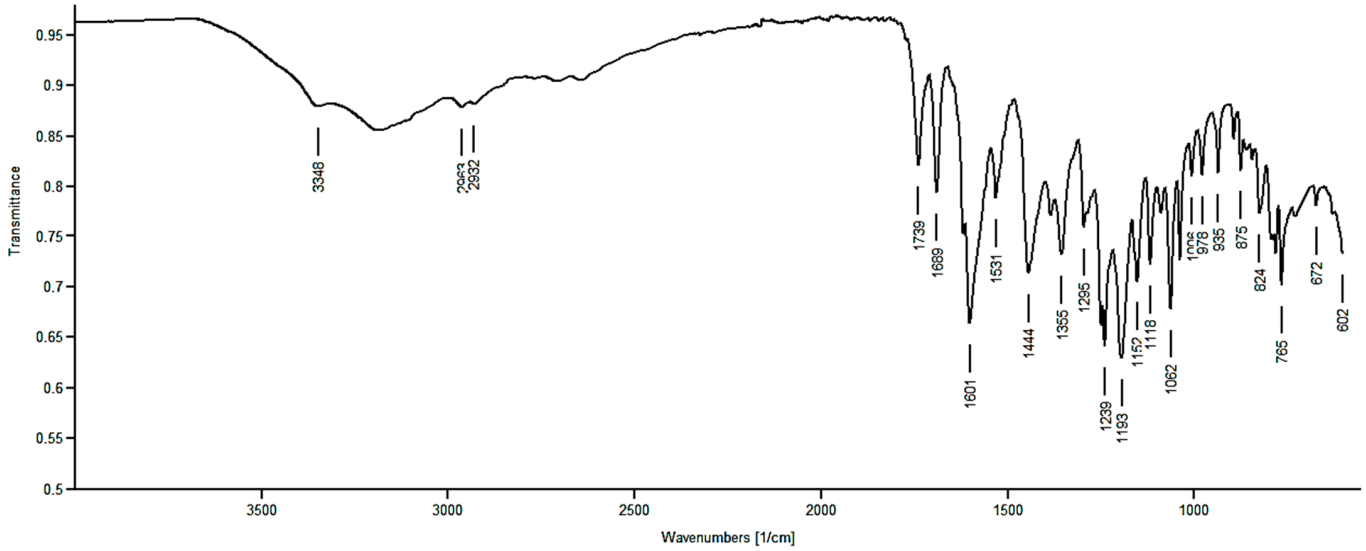

Figure 2. ATR–FTIR spectrum of CA.

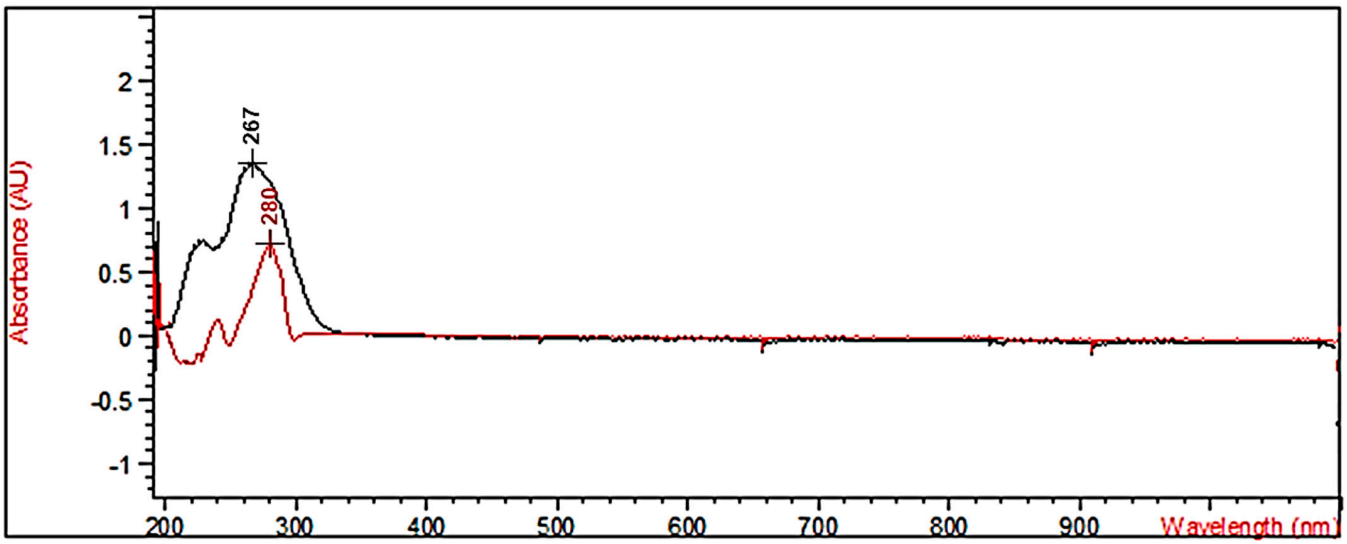

Figure 3. UV–Vis spectra of CA (black line) and (+)-catechin (red line).

Although the results obtained by us from UV–Vis and ATR–FTIR analyses cannot be compared with those obtained by Iobbi and collaborators, since such investigations were not carried out at all, they conformed to those reported by Sears et al. (UV–Vis and FTIR) [5] and Kennedy et al. (UV–Vis) [18]. The slight shift in the λ_{max} of the UV–Vis analysis of CA (267 nm vs. 285 nm) is probably due to the different solvents used in the acquisition (MeOH vs. H_2O). In particular, in the UV–Vis spectra of CA and (+)-catechin (Figure 3), peaks with very similar shapes were observed, due to the strong structural correlation existing between the two molecules. On the contrary, different values of λ_{max}, indicating the presence of different chromophores and confirming the pureness of CA, were detected. Similar to Sears, we observed decomposition for temperatures over 190 °C, and elemental analysis provided results in the range of acceptability, further confirming the pureness of CA. Concerning the NMR spectra of CA, the ^{1}H NMR signals observed by us in the

spectrum acquired in CD_3OD were in accordance with those recently reported [8], which are in turn in compliance with those reported previously [13], with minor differences probably due to the different solvents [13] and the instruments' potency [8,13]. On the contrary, the signal of C-4 in the ^{13}C NMR observed by us was at a chemical shift considerably lower (higher fields) than that reported by Hashida [13] and recently provided [8] (152 ppm vs. 182.08 [13] or 189.1 [8]), but in accordance with the value reported by Navarrate et al. and with the keto–enol structure of CA [17]. Nonetheless, the higher values observed by the other authors are also acceptable, since they can be justified by the existence of an enol–enol tautomerism in the crystalline keto–enol structure of CA [19]. Figure 4 shows both the UHPLC–MS/MS analysis of CA and of (+)-catechin, having Rt = 0.87 min and 1.98, respectively, as well as the level of pureness of CA (only 4% of residual (+)-catechin is present in the CA sample), thus further confirming the quality of the CA prepared by us.

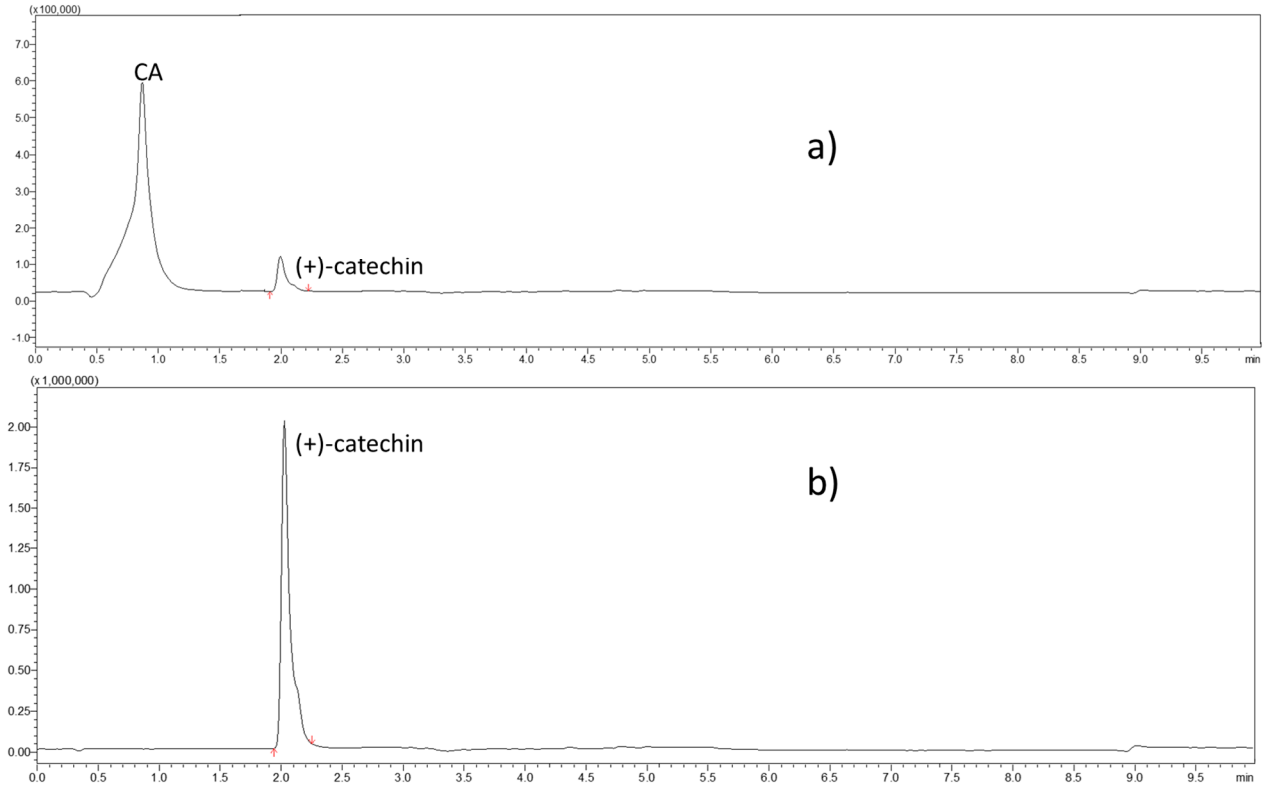

Figure 4. UHPLC–MS/MS chromatograms of CA solution at 250 ng/mL (**a**) and of (+)-catechin solution at 250 ng/mL (**b**).

2.2. Preparation of AOCA and Search for the Presence of 4-HBA

Starting from CA, we prepared AOCA by reproducing exactly the protocol developed in the past by Ferrea et al. [5] and recently reproduced by Iobbi and coworkers [8]. AOCA was obtained as a dark brown solid, as observable in Figure S2 (Section S1 SM). Additionally, while neither the AOCA prepared by Ferrea et al. [5] nor that prepared by Iobbi et al. [8] were completely characterized in terms of physicochemical analyses, we characterized it by TLC, ATR–FTIR, UV–Vis and UHPLC–MS/MS.

In particular, we prepared AOCA and analyzed it by several analytical techniques to unequivocally verify the accuracy of what was established by Iobbi and collaborators, who indicated compound **2** (identified by them as 4-HBA) as the main constituent of AOCA and responsible for its good antiviral activity, although on a virus different from the one originally studied by Ferrea to demonstrate the antiviral activity of AOCA [5]. It should be noted that **2**, i.e., the alleged 4-HBA, has been shown to be active by Iobbi et al. on a completely different type of virus (i.e., on ToBRa, a naked RNA virus) compared to the one on which the AOCA was originally found to be active (i.e., HSV-1 and HSV-2, DNA

viruses, coated with an envelope), but a commercial sample of 4-HBA was not analogously tested to confirm the identity attributed to **2**. As previously anticipated, there were several reasons that forced us to carry out the study described in this paper, which are briefly summarized in the following. In addition to the lack of literature reporting 4-HBA as a constituent, at least in trace amounts, of the products of the alkaline oxidation of catechin or CA [9–13], and to the several literature studies that describe the remarkable stability of the CA nucleus under the alkaline oxidative conditions [16], after careful examination, it appears that the works cited by Iobbi and coauthors to justify the presence of 4-HBA in AOCA do not confirm their discovery but, on the contrary, refute it [14,15]. Moreover, since we believed that analyses such as HPLC or at least TLC, highlighting the actual presence of 4-HBA in AOCA, were necessary, they were herein carried out by us. In fact, although the authors used semi-preparative HPLC to purify CA and to isolate **2** and reported the retention times (Rt) of the compounds [8], an HPLC analysis of AOCA that revealed exactly its composition was missing. Moreover, the determination of the melting point range of the isolated substance (**2**) to confirm its identity with 4-HBA was not performed. Furthermore, the results from NMR analysis carried out to identify the isolated material [8] (Supplementary Materials), in our opinion, are questionable and the spectra are not totally in accordance with those known for commercial samples of 4-HBA. In particular, even if, in the ^{1}H NMR spectrum of **2**, signals compatible with the AA'XX' system of the *p*-disubstituted phenyl ring of 4-HBA are observable at 7.87 ppm (d, 2H, J = 8.00 Hz, CH (2/6)) and 6.82 ppm (d, 2H, J = 8.01 Hz, CH (3/5)), other, not negligible signals are present at 0.5–1.5 ppm (particularly 0.8 and 1.5 ppm), which are missing in the spectrum of a commercial sample of 4-HBA (Figure 5), and which have not been justified at all by the authors [8].

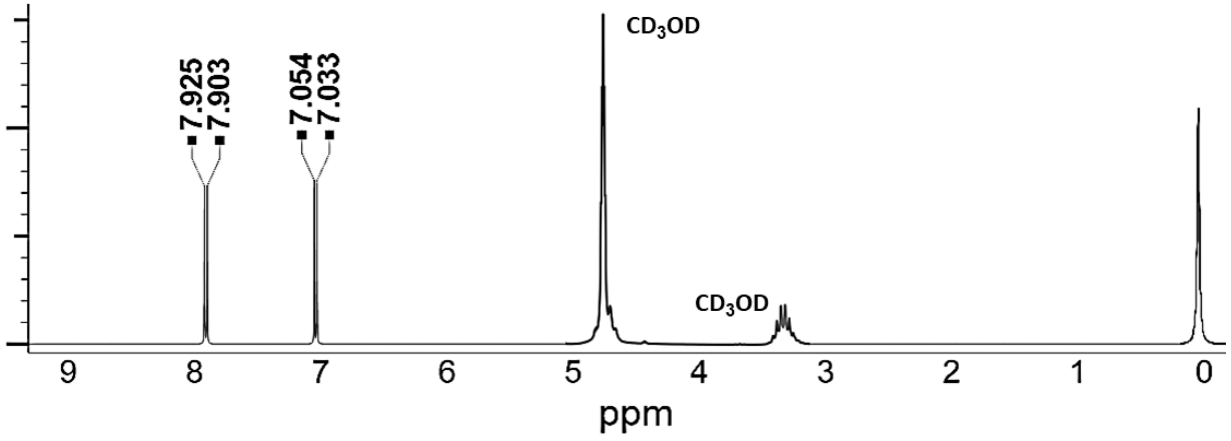

Figure 5. ^{1}H NMR spectrum (CD_3OD) of a commercial sample of 4-HBA.

For the precise assignment of the signals of the AA'XX' system observable in the ^{1}H NMR spectrum of **2**, which could be compatible with the structure of 4-HBA, and whose ^{13}C NMR has not been provided except in the form of a peak list in the main text, the authors carried out HSQC and HMBC 2D experiments (Supplementary Material) [8]. As far as we know, in an HSQC spectrum, a ^{13}C spectrum is displayed on one axis and a ^{1}H spectrum is displayed on the other axis, and cross-peaks show which proton is attached to which carbon considering only C-H (only one-bond coupling). Meanwhile, two-, three-, or sometimes even four-bond couplings are signaled in an HMBC spectrum. In particular, H-C-C or H-C-C-C, or even H-C-C-C-C, and not H-C, are visible. Regarding this, in the HSQC spectrum of **2**, one-bond couplings between the proton atom(s) at 1.5 ppm with carbon(s) having signals in the range 20–40 ppm are visible, which are not compatible with the structure of 4-HBA, and which have not been justified at all by Iobbi and coworkers [8]. Furthermore, it is of concern that, since it was assumed that **2** could be 4-HBA, the ^{1}H NMR spectrum was acquired in deutero methanol (which does not allow one to see the signals of

exchangeable protons, thus losing valuable information) rather than in deutero dimethyl sulfoxide. The dimethyl sulfoxide spectrum would have instead allowed the authors to confirm or refute the presence of the COOH and OH groups of 4-HBA.

Finally, differently from 2 (identified as 4-HBA) [8], a sample of commercial 4-HBA tested by us on VERO cells infected by HSV-2 was not active.

Based on these considerations, to verify the actual presence of 4-HBA among AOCA constituents, we examined the AOCA prepared by us, performing different analytical techniques, including the analyses missing in the paper recently published [8], and considered it essential to confirm or reject the identity assigned to **2**. In the following section of this article, the performed analyses, the results, and a brief discussion are given.

2.2.1. TLC Analyses of AOCA and 4-HBA

Employing aluminum-backed silica gel plates and detecting the spots at 254 nm and 365 nm, TLC analyses were carried out on AOCA and commercial 4-HBA, taken as a reference compound, using a mixture EtOAc/MeOH/AcOH 9/1/0.2 *v/v/v* (mixture A) as an eluent. Images of TLC are provided both in Figure 6a (AOCA on the left side of the TLC, 4-HBA on the right side) and in Section S2 of SM (Figure S5). Additionally, in Figure 6b, the TLC profile of AOCA obtained using MeOH 100% (mixture B) is included.

(**a**)

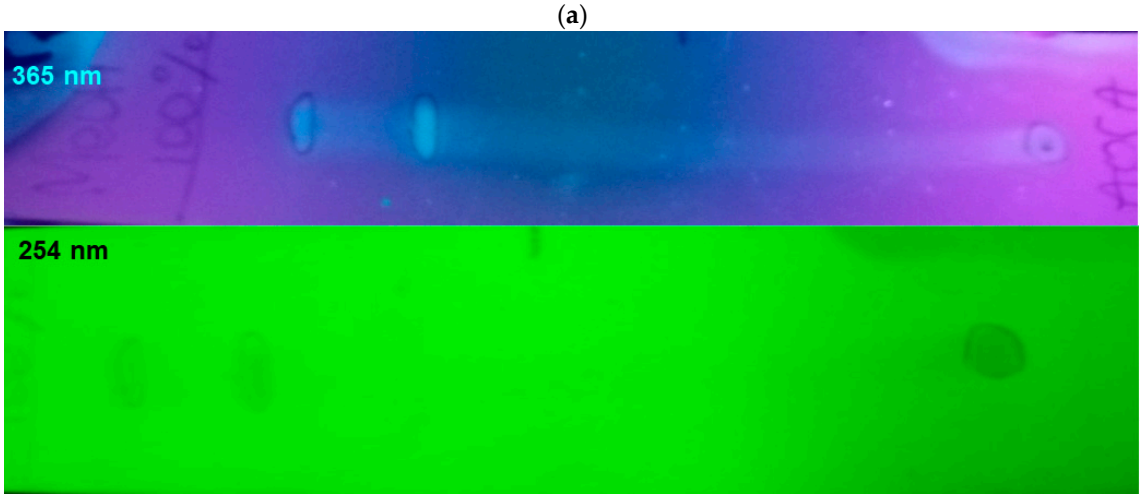

(**b**)

Figure 6. TLC analysis of AOCA (left side) and 4-HBA (right side), taken as reference compound (detection at 365 nm), showing the absence of 4-HBA in AOCA (**a**); TLC analysis of AOCA using MeOH 100% as eluent, showing the presence of two main groups of compounds (**b**).

As observable in both Figure S5 (254 nm) and Figure 6a (365 nm), there is no trace in AOCA of a spot corresponding to the Rf of 4-HBA, thus indicating the absence of 4-HBA in AOCA and the inaccuracy of the structural attribution suggested for **2** by Iobbi and collaborators [8].

2.2.2. UV–Vis Analyses of AOCA and 4-HBA

The UV–Vis spectra of AOCA and of a sample of commercial 4-HBA, taken as a reference compound, were acquired in MeOH, as described in the Materials and Methods section. The obtained spectra are reported in Figure 7. Additionally, in SM, an image showing the overlapped spectra of (+)-catechin, CA, AOCA, and 4-HBA is provided for the comparison of the UV–Vis profiles of all compounds considered in this study (Figure S6).

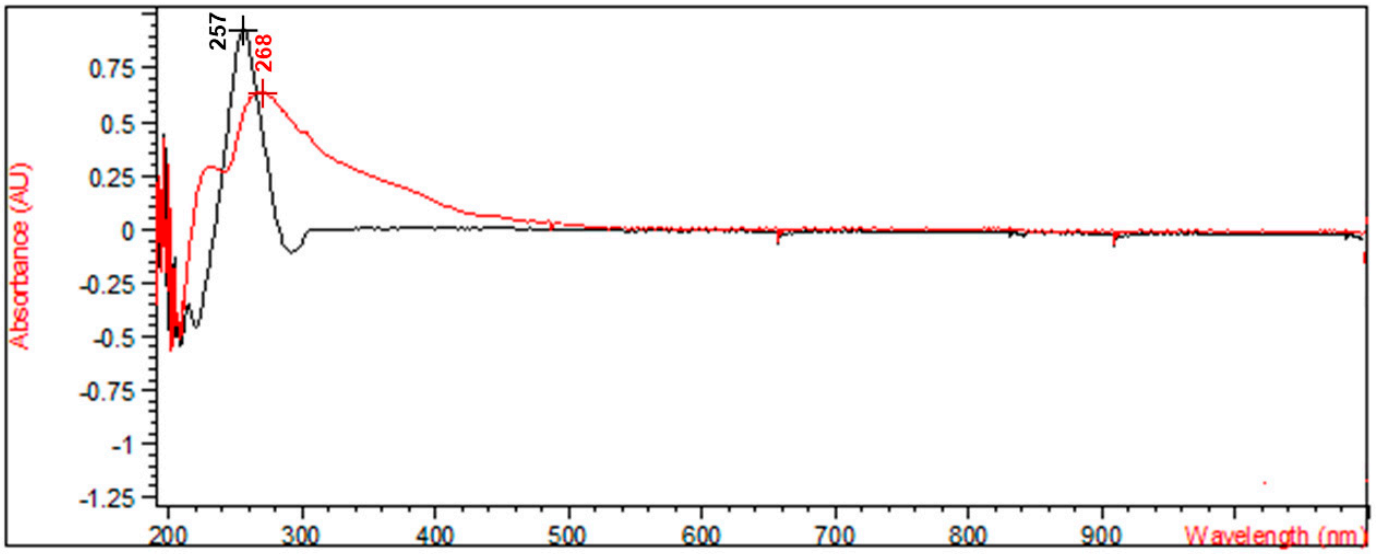

Figure 7. UV–Vis spectra of AOCA (red line) and 4-HBA (black line), taken as reference compound.

As Figure 7 and Figure S6 show, in the AOCA spectrum (λ_{max} = 268 nm), no peak is detectable at λ_{max} = 257 nm, corresponding to 4-HBA absorbance, while, considering the recently reported high concentration of **2** in AOCA (75% *wt/wt*), if this had been the case, a significant absorption at λ_{max} = 257 nm should have been observed in AOCA. This is further evidence that the structural attribution suggested for **2** is incorrect. Additionally, both concerning the shape and the λ_{max}, the UV–Vis spectra of CA and AOCA (Figures 3, 7 and S6), are very similar to each other, evidencing a strong structural correlation existing between the two molecules, and the presence of identical chromophores, suggesting that the nucleus of CA was maintained in AOCA. This agrees with what is widely reported, which asserts the presence of dimers of CA derivatives in the product of the oxidation of CA, rather than small phenolic molecules, such as 4-HBA. Furthermore, the very broad peak of AOCA suggests the presence either of several substances, as is typical of plant extracts [20], or of macromolecules, such as dimers and oligomers of CA [21], in different concentrations, rather than the presence of a small molecule such as 4-HBA at a concentration of 75%, whose UV peak appears much narrower.

2.2.3. UHPLC–MS/MS Analyses of (+)-Catechin, CA, AOCA, and 4-HBA

To obtain the best selectivity and specificity, a mass spectrometer equipped with a triple quadrupole analyzer as a detector was employed. An SRM method was built, monitoring three transitions for each analyte in ESI negative ion mode.

UHPLC–MS/MS analysis of standard solutions of CA, 4-HBA, and (+)-catechin were carried out as described in the Materials and Methods section, and the related chromatographic peaks eluted at Rt of 0.87, 1.86, and 1.98, respectively (Figure 8a). Then, a UHPLC–MS/MS analysis of the AOCA sample was performed (Figure 8b): there were several peaks, and their identification was not within our scope, but, unequivocally, no peak, even in trace, related to 4-HBA (magenta trace) was detectable (LOD = 0.3 ng/mL), highlighting the incorrect attribution suggested for the isolated material, whereas CA (at Rt = 0.87) was determined at a concentration of 15.8 ± 1.1 mg/g of AOCA.

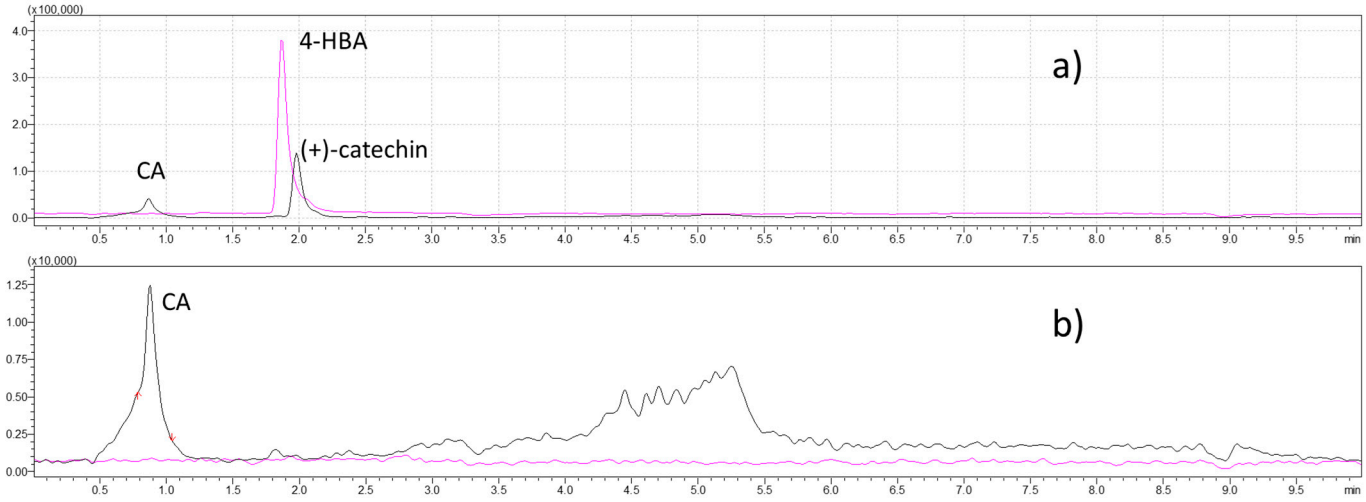

Figure 8. UHPLC–MS/MS chromatograms of mixture of CA, 4-HBA, and (+)-catechin (each at 100 ng/mL) (**a**) and AOCA sample (1000 ng/mL) (**b**). The black trace indicates the total ion current as the sum of the SRM transitions of CA and (+)-catechin, whereas the magenta trace indicates the total ion current as the sum of the 3 SRM transitions of 4-HBA.

2.2.4. Chemometric-Assisted ATR–FTIR Analyses of (+)-Catechin, CA, AOCA, and 4-HBA

ATR–FTIR spectra of commercial samples of (+)-catechin and 4-HBA, as well as of CA and AOCA prepared by us, were recorded, as described in the Materials and Methods section. The obtained spectra are available in Figure S7 ((+)-catechin), Figure S8 (CA), Figure S9 (AOCA), and Figure S10 (4-HBA) in Section S2 of SM. Moreover, in the subsequent Figure 9 are shown all the overlapped spectra (Figure 9a) and a magnification of a significant region of all the spectra (Figure 9b), to highlight similarities and differences among all the substances.

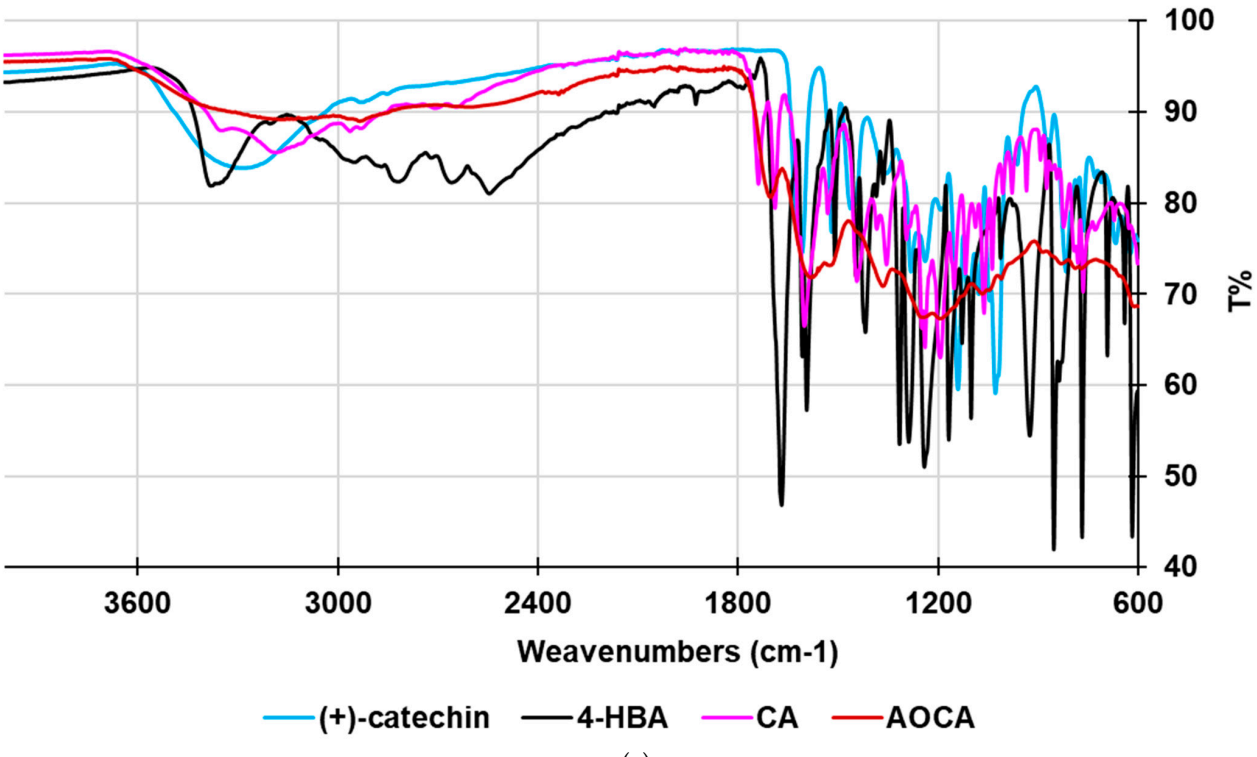

(**a**)

Figure 9. *Cont.*

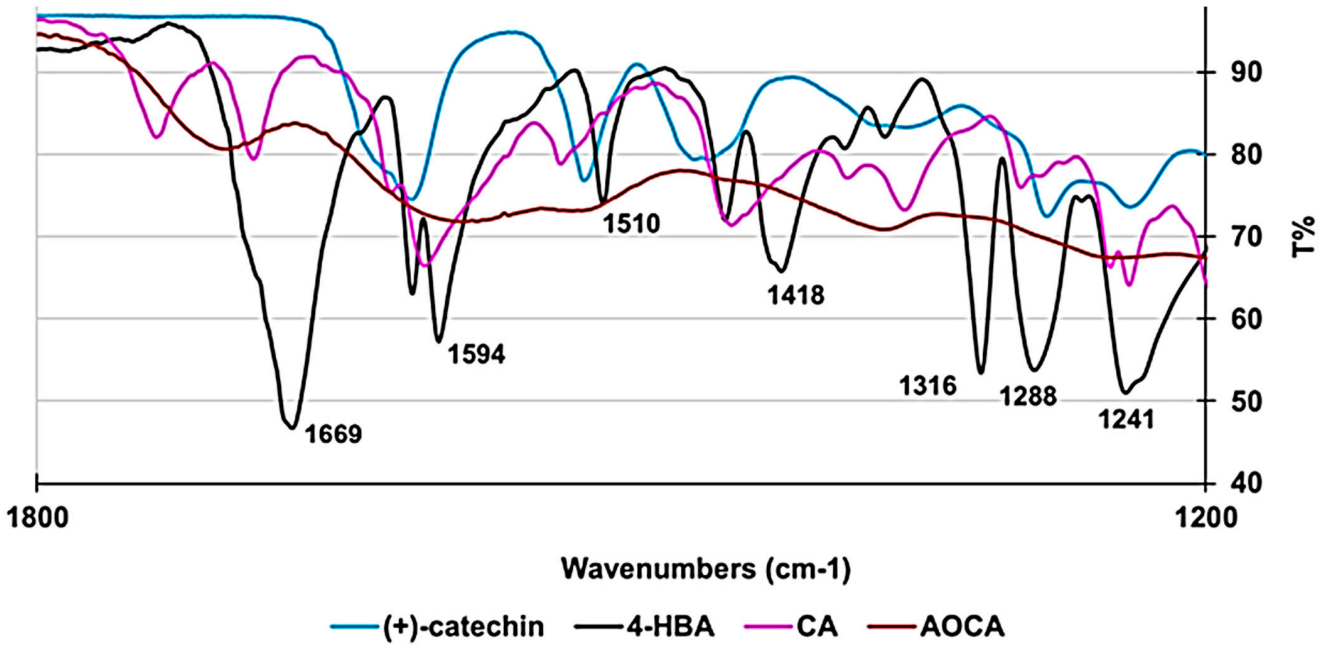

(**b**)

Figure 9. ATR–FTIR spectra of all samples (**a**) and magnification of a significant region with the wavenumbers (cm^{-1}) of significant bands belonging to 4-HBA and absent in AOCA (**b**).

From a simple observation of the spectra of AOCA and 4-HBA, none of the intense bands specific to 4-HBA (1669, 1594, 1510, 1418, 1316, 1288, and 1241 cm^{-1}), are detectable in the AOCA spectrum, while, if 4-HBA was **2**, isolated at 75% in AOCA, as reported [8], at least traces of such bands should have been detectable. Moreover, although merely by observing the ATR–FTIR spectra in Figure 9, the absence of 4-HBA in AOCA is unequivocal, we further confirmed this fact by processing the matrix of the ATR–FTIR spectral data of all samples using principal components analysis (PCA) [22–26]. PCA is a technique used in multivariate analysis (MVA), to process spectral data consisting of thousands of variables that need reduction to a smaller number of new variables, called principal components (PCs), which efficiently represent data variability in low dimensions. As a result, PCA provides score plots, where one component (e.g., PC1) is displayed vs. another (e.g., PC2), and where the samples under study assume specific positions (scores), forming groups of similar compounds. The position taken by each sample on the selected component can give predictive information on its chemical composition. Practically, compounds that are structurally similar will have similar scores and will be located close together, while compounds that are structurally different will have different scores and will be located distant from one another in the score plot. The PCA results allowed us to obtain the reciprocal positions of (+)-catechin (CAT), CA, AOCA, and 4-HBA occupied in the score plot of PC1 vs. PC2 (Figure 10).

All samples were well separated mainly on PC2 and reciprocally located at specific score values depending on their structural features. It was thus clearly evidenced that (+)-catechin, CA, and AOCA were positioned in the same square and at positive similar scores, thus testifying to their belonging to the same structural family, especially in the case of CA and AOCA. On the contrary, 4-HBA was positioned very distant from these compounds, at highly negative score values, thus confirming the strong structural differences between 4-HBA and AOCA, and the total absence of 4-HBA in AOCA.

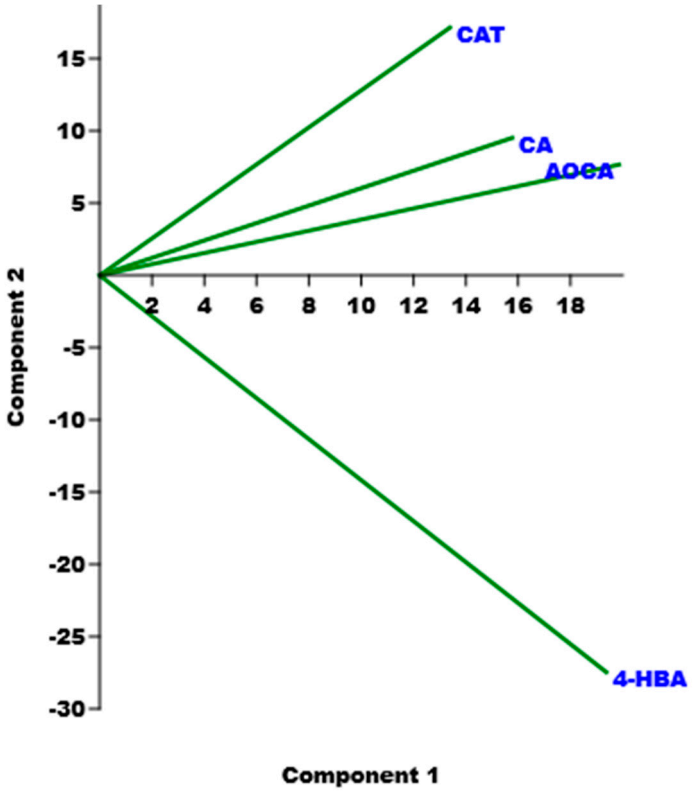

Figure 10. Principle component analysis (PCA) results are represented as a score plot implemented on the matrix collecting spectral data of (+)-catechin (CAT), CA, AOCA, and 4-HBA.

2.3. Evaluation of the Antiherpetic Effects of AOCA on HSV-2 In Vitro

To verify that the AOCA prepared by us, and that of Ferrea et al. [5], who found AOCA active against HSV-1 and HSV-2, were comparable, thus validating our findings, differently from Iobbi et al. who did not verify the goodness of their AOCA, we repeated, with AOCA on VERO cells the same tests carried out by Ferrea. In addition, hoping to highlight an antiviral activity of 4-HBA (the alleged 2) right on HSV-2, the same experiments were conducted with a commercial sample of 4-HBA.To this end, VERO cells were cultured as previously reported [5], while HSV-2 G strain was used to create viral infections in cells, as described by Ferrea and collaborators [5]. The results of these experiments reproduced those obtained by Fer-rea et al., thus establishing that even the AOCA prepared by us possessed dose-dependent activity against HSV-2. On the contrary, the commercial sample of 4-HBA, tested in the same conditions, was completely inactive also at very high concentrations against HSV-2. In particular, in standard plaque forming assay experiments, AOCA showed significant activity, and approximately 100% reduction in plaque formation in comparison with un-treated cultures was obtained at 8.0 μg/mL.

3. Materials and Methods

3.1. Chemical Compounds and Instruments

(+)-Catechin analytical standard from Sigma-Aldrich®, of plant origin, was purchased from Merck (Darmstadt, Germany). All reagents were of analytical grade and purchased from Merck (Darmstadt, Germany). Solvents were purified by standard procedures, whereas reagents were employed as such, without further purification. The melting range of CA was determined on a 360 D melting point device, resolution 0.1 °C (MICROTECH S.R.L., Pozzuoli, Naples, Italy), while ^{1}H and ^{13}C NMR spectra were acquired on a Jeol 400 MHz spectrometer (JEOL USA, Inc., Peabody, MA, USA) at 400 and 100 MHz, respectively. Fully decoupled ^{13}C NMR spectra were acquired. Chemical shifts were reported in ppm (parts per million) units relative to the internal standard tetramethylsilane (TMS = 0.00 ppm),

and the splitting patterns were described as follows: s (singlet), d (doublet), t (triplet), q (quartet), and m (multiplet), and br was added for broad signals. Elemental analyses were performed on an EA1110 Elemental Analyser (Fison Instruments Ltd., Farnborough, Hampshire, England). Organic solutions were evaporated using a rotatory evaporator, Rotavapor® R-3000 (Buchi, Cornaredo, Milan, Italy), operating at a reduced pressure of approximately 10–20 mmHg. Silicagel LC60A, 40–63 micron, purchased from Fluorochem Ltd. (Hadfield, Derbyshire, UK), was used for silica gel plugs.

Ultra-performance liquid chromatography coupled with tandem mass spectrometry (UHPLC–MS/MS) was employed in selected reaction monitoring (SRM) mode to identify the possible presence of 4-HBA in the AOCA sample. The LC/MS analyses were performed using the Nexera Liquid Chromatography Shimadzu (Kyoto, Japan) system, equipped with a DGU-20A3R degasser, two LC-30AD pumps, a SIL-30AC autosampler, a CTO-20AC column compartment, and a CMB-20 system. The system was interfaced with an LC-MS 8060 triple quadrupole mass spectrometer (Shimadzu, Kyoto, Japan) by an ESI ion source. The LC/MS data were acquired and processed with LabSolutions LCMS ver. 5.99 (Shimadzu Corporation, Kyoto, Japan) and LabSolutions Insight ver. 3.7 (Shimadzu Corporation, Kyoto, Japan) software.

3.2. Preparation of Catechinic Acid (CA)

Catechinic acid (CA) was prepared following the method described by Sears et al. [7]. In particular, (+)-catechin (Rf. = 0.82, ethyl acetate (EtOAc)/methanol (MeOH)/acetic acid (AcOH) 9/1/0.2 *v/v/v*) (1.0 g, 3.45 mmol) was added to a refluxing solution of 0.5% NaOH and stirred for 45 min. The dark solution was then cooled in ice and treated with Amberlite IR-120 resin (H+ form) (Merck, Darmstadt, Germany), and stirred for 1 h. The resin was then filtered off, and the solution was evaporated to dryness to give a dark brown oil, which was purified first by filtration through a silica gel plug (h = 20 cm, Ø = 2 cm) using a mixture of EtOAc/MeOH/AcOH (54/6/1.2 *v/v/v*) as an eluent. The solvent was then removed at reduced pressure (t = 60 °C) to obtain an orange solid, which was treated with ethyl ether (Et_2O) and filtered. The obtained solid was further purified by crystallization (acetone/Et_2O), washed with Et_2O three times, and brought to a constant weight at vacuum (0.6927 g, 2.02 mmol).

Catechinic acid (CA). Isolated yield 69.2%. Rf. = 0.26 (EtOAc/MeOH/AcOH 9/1/0.2 *v/v/v*). Mp.: >190 °C (charring.). ATR–FTIR (ν, cm^{-1}) 1745 (C = O); 1695, 1610, 1535. ^{1}H NMR (CD_3OD, 400 MHz, δ ppm) 2.06 (1H, ddd, H-8a, *J* = 14.23, 10.25, 2.73 Hz), 2.13 (1H, ddd, H-8b, *J* = 14.23, 2.84, 2.63 Hz), 3.39 (1H, dd, H-6, *J* = 10.25, 2.73 Hz), 3.76 (1H, dd, H-1, *J* = 2.84, 2.73 Hz), 3.90 (1H, d, H-5, *J* = 2.73 Hz), 5.12 (1H, td, H-7, *J* = 10.25, 2.84 Hz), 5.95 (1H, s, H-3), 6.69 (1H, d, H-6′, *J* = 8.52 Hz), 6.74 (1H, d, H-5′, *J* = 8.52 Hz), 6.80 (1H, s, H-2′).

^{13}C NMR (100 MHz, δ ppm) 212.7 (C = O, C9), 199.5 (C = O, C2), 152.5 (COH, C4), 146.3 (COH, C4′), 145.8 (COH, C3′), 139.2 (C, C1′), 128.7 (CH, C5′), 115.8 (CH, C4′), 114.8 (CH, C2′), 104.5 (CH, C3), 69.3 (CHOH, C7), 73.8 (CH, C1), 58.8 (CH, C1), 40.7 (CH C5,6), 32.5 (CH2, C8). Anal. Calcd. for $C_{15}H_{14}O_6$: C, 62.07%; H, 4.86%; O, 33.07%. Found: C, 62.37%; H, 4.90%; O, 33.00%.

3.3. Alkaline Autoxidation of CA

CA was then subjected to alkaline autoxidation, as previously described [5]. Briefly, in a three-necked flask equipped with a condenser, a thermometer, and a magnetic stirrer, an alkaline solution was prepared by dissolving 0.5 g NaOH in 7.5 mL of water. CA (0.5342 g, 1.84 mmoL) was added, and the dark brown solution was stirred for 30 min at room temperature, and then for another 30 min at 55 °C, and, finally, for 1.5 h at 100 °C. After cooling, the black solution was passed through Amberlite IR-120 (H+ form) (Merck, Darmstadt, Germany), an ion exchange resin column (h = 5 cm, Ø = 1 cm), and evaporated at reduced pressure to dryness, obtaining AOCA (0.5753 g) as a deep dark brown solid (AOCA).

3.4. TLC Analyses of (+)-Catechin, CA, AOCA, and 4-HBA

Thin-layer chromatography (TLC) was carried out employing aluminum-backed silica gel plates (Merck DC-Alufolien Kieselgel 60 F254, Merck, Washington, DC, USA), and detecting spots by UV light (254 nm or 365 nm), using a handheld UV lamp, LW/SW, 6W, UVGL-58 (Science Company®, Lakewood, CO, USA). The chromatographs were eluted in a closed glass developing chamber to keep the environment saturated with solvent vapors, using a mixture of EtOAc/MeOH/AcOH 9/1/0.2 *v/v/v* (mixture A) or 100% MeOH (mixture B).

3.5. UV–Vis Analyses of (+)-Catechin, CA, AOCA, and 4-HBA

The UV–Vis spectra of (+)-catechin, CA, AOCA, and 4-HBA were acquired using a UV–Vis spectrophotometer (HP 8453, Hewlett Packard, Palo Alto, CA, USA) equipped with a 3 mL cuvette. With the use of a microbalance, amounts of (+)-catechin, CA, AOCA, and 4-HBA were exactly weighted, solubilized in MeOH (50 mL), and appropriately diluted with the same solvent, obtaining solutions at the concentrations reported in Table 1. The obtained solutions were used for the analyses, recording the ultraviolet absorption spectra of all samples in the range 230–650 nm. Data of the analyses are included in Table 1.

Table 1. UV–Vis analyses of (+)-catechin, CA, AOCA, and 4-HBA.

Sample	(mg/mL)	λ_{max} (nm)	Abs (AU)
(+)-catechin	0.00482	289.0	0.72128
CA	0.00876	267.0	1.35380
AOCA	0.00462	268.0	0.64020
4-HBA	0.00653	257.0	0.93378

3.6. UHPLC–MS/MS Analyses of (+)-Catechin, CA, AOCA, and 4-HBA Standard Solutions

The stationary phase involved a Raptor Biphenyl column (100 × 2.1 mm, 1.8 µm) acquired from Restek (Milan, Italy), and a Raptor Biphenyl UHPLC (5 × 2.1) was used as a guard column. The mobile phase was a mixture of (A) ultrapure water and (B) methanol, both with the addition of 0.02% of acetic acid, eluting under the following gradient conditions: 0.0–0.3 min 10% B, 0.3–5.0 min 100% B, 5.0–8.0 min 100% B, 8.1 min 10%. B. The final run time was 10.0 min. The flow rate was 0.45 mL min^{-1}, the injection volume was 1.0 µL, and the oven temperature was set at 45 °C.

The ESI worked in negative polarity ion mode (NI) and the mass spectrometer was used in selected reaction monitoring (SRM) mode. The optimized instrumental parameters were set as follows: nebulizing gas flow 3.0 L/min; heating gas flow 10 L/min; drying gas flow 10 L/min; interface temperature 300 °C; DL temperature 250 °C; heat block temperature 400 °C. The unit mass resolution was established and maintained in each mass-resolving quadrupole by keeping a full width at half-maximum (FWHM) of approximately 0.7 u. The SRM transitions with the related dwell times and the optimized compound-dependent parameters, such as voltage potential Q1, Q3, and collision energy (CE), are reported in Table S1 in the Supplementary Materials (SM).

3.7. Chemometric-Assisted ATR–FTIR Analyses of (+)-Catechin, CA, AOCA, and 4-HBA

FTIR spectra of commercial samples of (+)-catechin and 4-HBA, as well as of CA and AOCA prepared by us, were recorded in attenuated total reflection (ATR) mode directly on the sample on a Spectrum Two FTIR Spectrometer (PerkinElmer, Inc., Waltham, MA, USA). The spectra were acquired in triplicate for each compound in the transmittance scale. The acquisition was made from 4000 to 600 cm^{-1}, with 1 cm^{-1} spectral resolution, coadding 32 interferograms, with a measurement accuracy in the frequency data at each measured point of 0.01 cm^{-1}, due to the laser internal reference of the instrument. The frequency of each band was obtained automatically by using the "find peaks" command of the instrument's software. The matrix created from the spectral data of all samples was subjected

to principal component analysis (PCA) using PAST statistical software (Paleontological Statistics software package for education and data analysis, freely downloadable online, at https://past.en.lo4d.com/windows, accessed on 3 June 2022). In particular, the FTIR dataset of the spectra acquired for (+)-catechin, 4-HBA, CA, and AOCA was arranged in a matrix of n measurable variables. For each sample, the variables consisted of the values of absorbance (%) associated with the wavenumbers (3401) in the range 4000–600 cm^{-1}. To simplify the system, we exploited PCA, which reduced the large number of variables to a small number of new variables, namely principal components (PCs). Chemometric analyses by PCA were performed on a matrix of data 4 × 3401, including a total of 13,604 original variables.

3.8. Antiherpetic Effects of 4-HBA and AOCA

African green monkey cells (VERO) (Flow Laboratories Ltd., Irvine, Scotland) were grown as previously reported [5], while HSV-2 strain G, kindly provided by Dr. R. Whitley (University of Alabama, Birmingham, AL), was stored at −70 °C until use. The antiviral activity of AOCA was determined following the procedure reported by Ferrea et al. [5]. In particular, monolayers of VERO cells in a 24-well Costar microplate (Bellco-Glass, Vineland, NJ, USA) were infected with 30 PFU of HSV-2 G strain with or without different concentrations of AOCA or 4-HBA. The plaque assay was performed as follows. Briefly, the virus was suspended either in RPM medium supplemented with 2% fetal calf serum or in six concentrations of AOCA or 4-HBA, and 1 mL aliquots of the suspensions were added to cell monolayers. After 1 h of absorption, the supernatant was aspirated and 1 mL of RPM medium containing 2% fetal calf serum and 0.5% human immune globulin and six different concentrations of AOCA or 4-HBA were added. Experiments were performed in quadruplicate. After 48 h of incubation at 37 °C in 5% CO_2, the medium was removed, and the plaque formation was determined microscopically after methanol fixation and staining with GIEMSA solution.

4. Conclusions

Compound **2** was recently isolated from the product of the oxidation of *Combretum* leaf extracts and catechinic acid (CA), namely AOCA. It was discovered to be active against ToBRFV and was identified as 4-HBA. Here, considering the identity reported for **2** very unlikely, and far from aiming to report new biological findings concerning AOCA or identify the constituents of AOCA, an unusual study has been reported, aimed at verifying the presence of 4-HBA among the constituents of AOCA (at a concentration above 50%) and its actual antiviral activity. To this end, we have prepared CA from (+)-catechin of plant origin and in turn we have prepared AOCA from CA. AOCA has been subsequently analyzed by performing TLC, UV–Vis, UHPLC–MS/MS, and chemometrically assisted ATR–FTIR experiments, unequivocally ascertaining that 4-HBA is not a constituent of AOCA, and that the structural attribution given to the antiviral compound **2** recently isolated from AOCA by Iobbi and collaborators is incorrect. As further confirmation, differently from AOCA prepared by us and AOCA prepared by Ferrea et al., a commercial sample of 4-HBA was completely inactive when tested on HSV-2. At this point, we wonder with great interest what is the actual identity of compound **2**, isolated from AOCA by Iobbi and collaborators and found endowed with antiviral activity against ToBRFV. Our greatest concern is that, having erroneously identified **2** as 4-HBA, Iobbi et al. have attributed to 4-HBA, completely free of any antiviral activity, relevant beneficial properties, deceiving the entire scientific community (and beyond), with possibly serious consequences for the health of humans and the environment due to the improper use of 4-HBA. The significant error made by Iobbi et al. and the present work evidence that, due to the diverse and complex material of plant derivatives, detailed studies and verification are necessary, as well as the development of new analytical methods.

Supplementary Materials: The following supporting information can be downloaded at: https://www.mdpi.com/article/10.3390/plants11141822/s1, Table S1. SRM NI transitions (Q1 and Q3 masses), dwell time, retention time (tR), and mass spectrometry parameters: Q1 Pre Bias, CE (Collision Energy), Q3 Pre Bias. The three most sensitive transitions for each species were monitored. Figure S1. TLC image observed at 254 nm (eluent ethyl acetate (EtOAc)/methanol (MeOH)/acetic acid (AcOH) 9/1/0.2 *v/v/v*). From the left: (+)-catechin (Rf. 0.82) and crude CA (Rf. 0.26); isolated CA and (+)-catechin; three samples of CA obtained by three different crystallizations from acetone/ethyl ether. Figure S2. Aspect of the crystallized CA (right) and of the product of alkaline autooxidation of CA (AOCA). Figure S3. ^{1}H NMR (CD_3OD, 400 MHz) spectrum of CA. Figure S4. ^{13}C NMR (CD_3OD, 100 MHz) spectrum of CA. Figure S5. TLC analysis of AOCA and 4-HBA, taken as reference compound (detection at 254 nm), showing the absence of 4-HBA in AOCA. Figure S6. UV–Vis spectra of (+)-catechin (blue line), CA (light-blue line), AOCA (red line), and 4-HBA (black line). Figure S7. ATR–FTIR spectrum of (+)-catechin. Figure S8. ATR–FTIR spectrum of CA. Figure S9. ATR–FTIR spectrum of AOCA. Figure S10. ATR–FTIR spectrum of 4-HBA.

Author Contributions: Conceptualization, methodology, software, validation, formal analysis, investigation, data curation, writing—original draft preparation, writing—review and editing, visualization, supervision, project administration, S.A.; UV–Vis analyses, G.Z.; writing—review and editing, UHPLC–MS/MS analyses, F.G.; biological assays, D.C. and S.P. All authors have read and agreed to the published version of the manuscript.

Funding: This research received no external funding.

Institutional Review Board Statement: Not applicable.

Informed Consent Statement: Not applicable.

Data Availability Statement: Data supporting the reported results are all presented in this manuscript or in the Supplementary Materials included.

Acknowledgments: The authors are very thankful to Carla Villa for having allowed us to use her HPLC instrument.

Conflicts of Interest: The authors declare no conflict of interest.

References

1. Welch, C.; Zhen, J.; Bassène, E.; Raskin, I.; Simon, J.E.; Wu, Q. Bioactive polyphenols in kinkéliba tea (*Combretum micranthum*) and their glucose-lowering activities. *J. Food Drug Anal.* **2018**, *26*, 487–496. [CrossRef] [PubMed]
2. Zhen, J.; Welch, C.; Guo, Y.; Bassène, E.; Raskin, I.; Simon, J.E.; Wu, Q. Novel skeleton flavan-alkaloids from African herb tea kinkéliba: Isolation, characterization, semisynthesis, and bioactivities. In *African Natural Plant Products, Volume III: Discoveries and Innovations in Chemistry, Bioactivity, and Applications*; ACS Symposium Series; American Chemical Society: Washington, DC, USA, 2020; Volume 1361, pp. 297–312.
3. D'Agostino, M.; Biagi, C.; De Feo, V.; Zollo, F.; Pizza, C. Flavonoids of *Combretum micranthum*. *Fitoterapia* **1990**, *61*, 477.
4. Tine, D.; Fall, A.D.; Dieng, S.I.; Sarr, A.; Bassene, E. Total polyphenol, tannin and flavonoid contents of *Combretum micranthum* leaves harvested in three regions of Senegal: Diass, Sandiara and Essyl. *Int. J. Biol. Chem. Sci.* **2019**, *13*, 1817–1820. [CrossRef]
5. Ferrea, G.; Canessa, A.; Sampietro, F.; Cruciani, M.; Romussi, G.; Bassetti, D. In vitro activity of a *Combretum micranthum* extract against *Herpes simplex* virus types 1 and 2. *Antivir. Res.* **1993**, *21*, 317–325. [CrossRef]
6. El Sayed, K.A. Natural products as antiviral agents. In *Studies in Natural Products Chemistry*; Attaur, R., Ed.; Elsevier: Amsterdam, The Netherlands, 2000; Volume 24, pp. 473–572.
7. Sears, K.D.; Casebier, R.L.; Hergert, H.L.; Stout, G.H.; McCandlish, L.E. Structure of catechinic acid. Base rearrangement product of catechin. *J. Org. Chem.* **1974**, *39*, 3244–3247. [CrossRef]
8. Iobbi, V.; Lanteri, A.P.; Minuto, A.; Santoro, V.; Ferrea, G.; Fossa, P.; Bisio, A. Autoxidation Products of the Methanolic Extract of the Leaves of *Combretum micranthum* Exert Antiviral Activity against *Tomato Brown Rugose Fruit Virus* (ToBRFV). *Molecules* **2022**, *27*, 760. [CrossRef]
9. Germann, D.; Stark, T.D.; Hofmann, T. Formation and characterization of polyphenol-derived red chromophores. Enhancing the color of processed cocoa powders: Part 1. *J. Agric. Food Chem.* **2019**, *67*, 4632–4642. [CrossRef]
10. Laks, P.E.; Hemingway, R.W.; Conner, A.H. Condensed tannins. Base-catalysed reactions of polymeric procyanidins with phloroglucinol: Intramolecular rearrangements. *J. Chem. Soc. Perkin Trans.* **1987**, *1*, 1875–1881. [CrossRef]
11. Ohara, S.; Hemingway, R.W. Condensed tannins: The formation of a diarylpropanol-catechinic acid dimer from base-catalyzed reactions of (+)-catechin. *J. Wood Chem. Technol.* **1991**, *11*, 195–208. [CrossRef]

12. Hashida, K.; Ohara, S. Formation of a novel catechinic acid stereoisomer from base-catalyzed reactions of (+)-catechin. *J. Wood Chem. Technol.* **2002**, *22*, 11–23. [CrossRef]
13. Hashida, K.; Ohara, S.; Makino, R. Base-Catalyzed Reactions of (−)-Epicatechin: Formation of Enantiomers of Base-Catalyzed Reaction Products from (+)-Catechin. *J. Wood Chem. Technol.* **2003**, *23*, 227–232. [CrossRef]
14. Newhall, W.F.; Ting, S.V. Degradation of hesperetin and naringenin to phloroglucinol. *J. Agric. Food Chem.* **1967**, *15*, 776–777. [CrossRef]
15. Niklas, K.J.; Giannasi, D.E. Geochemistry and thermolysis of flavonoids. *Science* **1977**, *197*, 767–769. [CrossRef]
16. Jensen, O.N.; Pedersen, J.A. The oxidative transformations of (+)catechin and (-)epicatechin as studied by ESR. *Tetrahedron* **1983**, *39*, 1609–1615. [CrossRef]
17. Navarrete, P.; Pizzi, A.; Bertaud, F.; Rigolet, S. Condensed tannin reactivity inhibition by internal rearrangements: Detection by CP-MAS 13C NMR. *Maderas. Cienc. Tecnol.* **2011**, *13*, 59–68. [CrossRef]
18. Kennedy, J.A.; Munro, M.H.G.; Powell, H.K.J.; Poter, L.J.; Foo, L.Y. The protonation reactions of catechin, epicatechin and related compounds. *Aust. J. Chem.* **1984**, *37*, 885–892. [CrossRef]
19. Kol'tsov, A.I.; Elkin, A.A.; Zheglova, D.K. 13C NMR spectra and enol—Enol tautomerism in crystalline keto—Enols. *J. Mol. Struct.* **1990**, *221*, 309–313. [CrossRef]
20. Chen, W.; Wang, X.; Chen, C. Characterization of nine traditional Chinese plant extracts with specific acid dissociation constants by UV-Vis spectrophotometry. *Anal. Methods* **2014**, *6*, 581–588. [CrossRef]
21. Nagarajan, S.; Nagarajan, R.; Braunhut, S.J.; Bruno, F.; McIntosh, D.; Samuelson, L.; Kumar, J. Biocatalytically Oligomerized Epicatechin with Potent and Specific Anti-proliferative Activity for Human Breast Cancer Cells. *Molecules* **2008**, *13*, 2704–2716. [CrossRef]
22. Alfei, S.; Brullo, C.; Caviglia, D.; Zuccari, G. Preparation and Physicochemical Characterization of Water-Soluble Pyrazole-Based Nanoparticles by Dendrimer Encapsulation of an Insoluble Bioactive Pyrazole Derivative. *Nanomaterials* **2021**, *11*, 2662. [CrossRef]
23. Alfei, S.; Zuccari, G.; Schito, A.M. Considerable Improvement of Ursolic Acid Water Solubility by its Encapsulation in Dendrimer Nanoparticles: Design, Synthesis and Physicochemical Characterization. *Nanomaterials* **2021**, *11*, 2196. [CrossRef] [PubMed]
24. Alfei, S.; Spallarossa, A.; Lusardi, M.; Zuccari, G. Successful Dendrimer and Liposome-Based Strategies to Solubilize an Antiproliferative Pyrazole Otherwise Not Clinically Applicable. *Nanomaterials* **2022**, *12*, 233. [CrossRef] [PubMed]
25. Alfei, S.; Oliveri, P.; Malegori, C. Assessment of the Efficiency of a Nanospherical Gallic Acid Dendrimer for Long-Term Preservation of Essential Oils: An Integrated Chemometric-Assisted FTIR Study. *Chem. Sel.* **2019**, *4*, 8891–8901. [CrossRef]
26. Alfei, S.; Marengo, B.; Domenicotti, C. Development of a fast, low cost, conservative and eco-friendly method for quantifying gallic acid in polymeric formulations by FTIR spectroscopy in solution. *Chem. Sel.* **2020**, *5*, 4381–4388.